Electron-electron scattering in strong magnetic fields in quantum well systems

K. Kempa, Y. Zhou, J. R. Engelbrecht, and P. Bakshi
Department of Physics, Boston College, Chestnut Hill, Massachusetts 02467, USA
(Received 27 November 2002; published 7 August 2003)

We have developed a theory of the electron-electron scattering in quantum well structures in the presence of a magnetic field. The scattering rate is obtained from the second-order expansion of the electron self-energy. We show that the rate oscillates as a function of the magnetic field, so that a strong suppression of the scattering can be expected in some ranges of high magnetic fields. Our theory also provides an easy tool for distinguishing this two-electron scattering process from other possible scattering mechanisms.

DOI: 10.1103/PhysRevB.68.085302 PACS number(s): 73.63.Hs, 72.10.−d

I. INTRODUCTION

The electron-electron scattering processes in homogeneous electron systems are well understood.[1] For quantum well systems, such scattering has been considered through simplified approaches,[2,3] as well as through a random-phase approximation (RPA) treatment which included effects of dynamical screening.[4,5] In this paper we examine the effects of an applied magnetic field on electron-electron scattering in quantum well systems.

Intersubband electron-electron scattering can be an important carrier relaxation channel in quantum nanostructures. This, for example, is the case in the current driven two subband GaAs quantum wells, with heavy injection into the upper and extraction from the lower subband, in which intersubband separation is less than 36 meV. This energy represents the onset of very strong relaxation though LO phonon excitations. Smaller subband separations imply that those excitations cannot be generated by electrons scattering between these subbands. In the absence of the electron-LO-phonon scattering, the intersubband electron-electron process can dominate the dynamics, or at least be comparable to the electron-defect scattering, if there is a sufficient electron density in the structure. This can be the case in structures used as active regions of devices designed for emission of radiation in the THz frequency range.[6–8] Knowledge of the electron-electron scattering rates is therefore crucial in determining the electrical and thermal transport properties of such structures. Typically, these operate in a nonequilibrium steady state, and in some cases carry a large electron population in the active region. Then the electron-electron scattering becomes an important factor to be considered for achieving population inversion. Of obvious interest here is the possibility of reducing those electron-electron scattering rates. One way to accomplish this is to apply a strong magnetic field in the growth direction of the quantum well structure. Classically, the electrons execute cyclotron orbits of small size, proportional to the inverse of the magnetic field; thus increasing B reduces the electron-electron scattering cross section. We have developed here a full quantum-mechanical treatment, and show that the electron-electron scattering is indeed reduced for large B. In addition, it oscillates as a function of B. Thus a reduction in scattering strength is achievable for particular ranges of the magnetic field.

Another important conclusion, arising from this oscillatory behavior, is the possibility of distinguishing between two-electron and single-electron scattering processes. We have already shown that this oscillatory behavior can be used as a diagnostic for the presence of (and comparative importance of) the electron-electron scattering in quantum well structures, as compared to other single-electron scattering processes.[9]

We develop the formalism for electron-electron scattering in the presence of B, in Sec. II, provide detailed computations and results for typical quantum well structures in Sec. III, and discuss the experimental implications and conclusions in Sec. IV.

II. FORMALISM

To investigate how Landau-level (LL) quantization of electron states affects electronic lifetimes, we develop a self-energy formalism for electron-electron transitions in the presence of a magnetic field.

The imaginary part of the self-energy provides the electron-electron scattering rate. Our earlier work on e-e scattering without a B-field led us to the conclusion that in many cases it is sufficient to work with only the first two diagrams[5,10] in the RPA expansion. We make a similar approximation here by using second-order perturbation theory. Since the first term is real, we need to consider only the second term. Using the Matsubara formalism, the second-order self-energy can be written as

$$\Sigma(\mathbf{r}_1,\mathbf{r}_2,i\omega_k)=\frac{1}{\beta}\sum_l \int_{\mathbf{r}_3,\mathbf{r}_4} G_0(\mathbf{r}_1,\mathbf{r}_2,i\omega_k+i\omega_l) \times v(\mathbf{r}_1,\mathbf{r}_3)\chi_0(\mathbf{r}_3,\mathbf{r}_4,i\omega_l)v(\mathbf{r}_4,\mathbf{r}_2), \quad (1)$$

where the electron Green's function is

$$G_0(\mathbf{r}_1,\mathbf{r}_2,i\omega_k)=\sum_m \frac{\psi_m(\mathbf{r}_1)\psi_m^*(\mathbf{r}_2)}{i\omega_k-E_m+\mu}. \quad (2)$$

Here ψ_m and E_m are the electron eigenfunctions and eigenvalues, $\omega_k=\pi(2k+1)k_BT$ and $\omega_l=\pi 2lk_BT$ are Fermi and Bose Matsubara frequencies, and $v(\mathbf{r}_1,\mathbf{r}_2)=e^2/\epsilon|\mathbf{r}_1-\mathbf{r}_2|$ with ϵ the dielectric constant of the semiconductor. Since we retain only the second-order contribution to the self-energy,

χ_0 is the bare bubble

$$\chi_0(\mathbf{r}_3,\mathbf{r}_4,\omega_l)=(-2/\beta)\Sigma_p G_0(\mathbf{r}_3,\mathbf{r}_4,\omega_p)G_0(\mathbf{r}_4,\mathbf{r}_3,\omega_p+\omega_l)$$

which reduces to

$$\chi_0(\mathbf{r}_3,\mathbf{r}_4,i\omega_l)=-2\sum_{m,p}\psi_p(\mathbf{r}_3)\psi_p^*(\mathbf{r}_4)\psi_m(\mathbf{r}_4)\psi_m^*(\mathbf{r}_3)\times\frac{[n_F(E_m)-n_F(E_p)]}{i\omega_l+E_m-E_p} \quad (3)$$

after performing[1] the fermion Matsubara sum $(1/\beta)\Sigma_p h(i\omega_p)=\Sigma_i R(z_i)n_F(z_i)$ where the function $h(z)$ has poles at complex frequencies z_i with residues $R(z_i)$. This introduces the Fermi occupation factors $n_F(E)=1/(e^{\beta(E-\mu)}+1)$. The remaining Matsubara sum in Eq. (1) can be performed in similar fashion, yielding

$$\Sigma(\mathbf{r}_1,\mathbf{r}_2,i\omega_k)=2\sum_{l,m,p}\int_{\mathbf{r}_3,\mathbf{r}_4}\psi_l(\mathbf{r}_1)\psi_l^*(\mathbf{r}_2)\psi_p(\mathbf{r}_3)\psi_p^*(\mathbf{r}_4)\times\psi_m(\mathbf{r}_4)\psi_m^*(\mathbf{r}_3)v(\mathbf{r}_1,\mathbf{r}_3)v(\mathbf{r}_4,\mathbf{r}_2)\times\frac{F_{p,m,l}}{i\omega_k+E_m-E_p-E_l+\mu}, \quad (4)$$

where the all-important level occupation of the intermediate states is accounted for by

$$F_{p,m,l}=n_F(E_m)[1-n_F(E_p)][1-n_F(E_l)]+[1-n_F(E_m)]n_F(E_p)n_F(E_l). \quad (5)$$

We now analytically continue $\Sigma(\mathbf{r}_1,\mathbf{r}_2,i\omega_k)$ to $\Sigma(\mathbf{r}_1,\mathbf{r}_2,\omega+i0^+)$ and then use $1/(x+i0^+)=\mathcal{P}1/x-i\pi\delta(x)$ to evaluate the imaginary part. The lifetime in state E_k due to electron-electron scattering is proportional to the expectation value,

$$\mathrm{Im}\langle\Sigma(\mathbf{r}_1,\mathbf{r}_2,E_k)\rangle=\int_{\mathbf{r}_1,\mathbf{r}_2}\psi_k(\mathbf{r}_1)\mathrm{Im}\,\Sigma(\mathbf{r}_1,\mathbf{r}_2,E_k)\psi_k^*(\mathbf{r}_2)=-2\pi\sum_{l,m,p}|V_{kl,mp}|^2F_{p,m,l}\times\delta(E_k+E_m-E_p-E_l), \quad (6)$$

where the transition amplitude is expressed in terms of the electron wave functions through

$$V_{kl,mp}=\int_{\mathbf{r},\mathbf{r}'}\psi_k^*(\mathbf{r})\psi_l(\mathbf{r})v(\mathbf{r},\mathbf{r}')\psi_m(\mathbf{r}')\psi_p^*(\mathbf{r}') \quad (7)$$

and one can define the total scattering rate out of state k,[1]

$$\gamma_k=\frac{4\pi}{\hbar}\sum_{l,m,p}|V_{kl,mp}|^2F_{m,p,l}\delta(E_k+E_m-E_p-E_l), \quad (8)$$

which could have been obtained from Fermi's golden rule as well, with proper inclusion of occupation factors.

The F factor in Eq. (8) has two terms. The first describes a physical process in which the ψ_k-state electron scatters into a hole and two electrons and the second term represents an electron and two holes in the intermediate state.

Now we consider a quantum well (QW) system, in which a magnetic field is applied in the z direction. The motion of electrons is given by

$$\frac{1}{2m}\left(\frac{\hbar}{i}\nabla-\frac{e}{c}\mathbf{A}\right)^2\psi(x,y,z)+V(z)\psi(x,y,z)=E\psi(x,y,z), \quad (9)$$

where $V(z)$ is the confining potential of the QW. We employ here the Landau gauge $\mathbf{A}=(0,Hx,0)$. The allowed electron wave functions are $\psi_{sl}(x,y,z)=\exp(i\beta_l y)\phi_s(z)u_l[x-x(\beta_l)]$ where s is the subband index, l the Landau level index, and β_l is a quasimomentum. The term $x(\beta_l)=\hbar\beta_l/m\omega_c$ in terms of the cyclotron frequency $\omega_c=eH/mc$ where the quantum number β_l is quantized in units $2\pi/L$, L being the sample size in the y direction. The wave function $u_l(x)=N_l\exp(-\alpha^2x^2/2)H_l(\alpha x)$ with H_l the Hermite polynomials and normalization $N_l=(\alpha 2^l l!/\sqrt{\pi})^{1/2}$ with $\alpha=\sqrt{c\hbar/eH}$. $\phi_s(z)$ is the solution to the one-dimensional (1D) Schrödinger equation,

$$-\frac{\hbar^2}{2m}\frac{d^2}{dz^2}\phi_s(z)+V(z)\phi_s(z)=\epsilon_s\phi_s(z), \quad (10)$$

and the electron energy is then $E=E_{sl}=(l+\frac{1}{2})\hbar\omega_c+\epsilon_s$. For each E_{sl} the states are degenerate with respect to β_l.

The main effect of the B field ($B=\mu_o H$) is that the subband electrons re-distribute between the multiply degenerate Landau levels. The inter-Landau-level separation decreases with B, so that for $B=0$ one recovers a continuum of states.

As an illustration of this formalism, consider a simple two subband scenario with $\Delta=\epsilon_2-\epsilon_1$. The energy conservation condition in Eq. (8) then introduces a strong constraint in the electron-electron intersubband scattering process. For $B\neq 0$ the Landau levels form in both subbands, and the electron-electron scattering vanishes when the argument of the delta function is nonzero. If we consider two electron transitions from the upper to the lower subband, the delta function argument represents the energy balance condition where the energy gain of one electron (for example, scattering from k to l), is balanced by the energy loss of the other (scattering from m to p). The argument of the delta function in Eq. (8) then vanishes (i.e., electron-electron scattering takes place) if

$$(l-k)+(p-m)=\frac{2\Delta}{\hbar\omega_c} \quad (11)$$

or

$$\hbar\omega_c=\frac{2\Delta}{n} \quad (12)$$

with $n=l-k+p-m$, an integer.

For a given intersubband separation Δ, such electron-electron scattering events can occur only for these quantized values of $B=B^*/n$ with $B^*=\mu_0 2\Delta mc/\hbar e$. The intersubband scattering rate for this process is given by [see Eq. (8)]

$$\gamma_{21,21}^k=\frac{4\pi}{\hbar}\sum_{l,p,m}|V_{kl,mp}|^2F_{m,p,l}\delta(2\Delta-\hbar\omega_c n) \quad (13)$$

with the matrix element

$$V_{kl,mp}=\int\int dxdx'\int\int dzdz'\phi_2^*(z)\phi_2(z')\phi_1(z)$$
$$\times\phi_1^*(z')u_k[x-x(\beta_k)]u_l[x'-x(\beta_l)]$$
$$\times u_m[x-x(\beta_m)]u_p[x'-x(\beta_p)]2e^2K_0[(\beta_k-\beta_m)$$
$$\times\sqrt{(x-x')^2+(z-z')^2}]\delta(\beta_k+\beta_m-\beta_p-\beta_l). \tag{14}$$

Note that each state represented by an index j in the general formalism of Eq. (8) has three indices, as explained below Eq. (9): the first is the band index s, the second is the Landau-level index j, and the third is the corresponding wave number β_j [see Eq. (9)]. Equations (13) and (14), for example, already have the specific bands $s=2,1$ indicated, and the matrix element indexes refer to the Landau-level indexes j, as well as, the corresponding set of quasimomenta β_j. j in the occupation factor F also refers to j and β_j, while n in the delta function is only composed of the Landau level indexes l,k,p, and m. The summation is over all states j and β_j, consistent with the delta function constraint. Carrying out the summations over the two final state indices β_l, β_p, and the initial state index β_m of the other electron, and averaging over the initial electron index β_k in Eq. (13), the scattering rate reduces to

$$\gamma_{21,21}^k=\frac{4\pi}{\hbar}\sum_{l,p,m}W_{kl,mp}G_{m,p,l}\delta(2\Delta-\hbar\omega_c n), \tag{15}$$

where the indices now refer only to the LL. The occupation factor G in Eq. (15) is given by

$$G_{m,p,l}=(\mu_m/\hbar\omega_c)(1-\mu_l/\hbar\omega_c)(1-\mu_p/\hbar\omega_c), \tag{16}$$

where $\mu_j/\hbar\omega_c$ is the population fraction on LL j. W is the result of integrating $|V|^2$ over the indices β_l, β_m, β_p and averaging over the initial state index β_k. Note that it is still dependent on the LL indices *klmp*.

III. NUMERICAL CALCULATIONS

As an example, we consider a two subband system where only the lowest Landau level of the upper subband is occupied, and the lower subband is empty. Such a scenario would be experimentally realized if there is narrow injection into upper subband, and heavy extraction from the lower subband.[9,11] We calculate the scattering rate using Eq. (15). The strength of the δ-function peak for a given n is given by

$$a_n=\sum_{lP}W_{0l,0p} \tag{17}$$

if we take the occupied LL to be full. The matrix element is evaluated employing the Gaussian integration for the $x-x'$ and $z-z'$ integration. In order to avoid singularities of K_0, we choose a set of Gaussian mesh points and weight factors as discrete values for summation. Also, we apply the condition of the overlap of wave functions in our system to significantly reduce our computing time. To find $\phi_s(z)$ we solve Eq. (9) for a realistic potential $V(z)$ of the experimental quantum well structure used in our $B=0$ calculations.[5] Various benchmark tests were carried out to check the numerical convergence and the accuracy of the numerical computations.

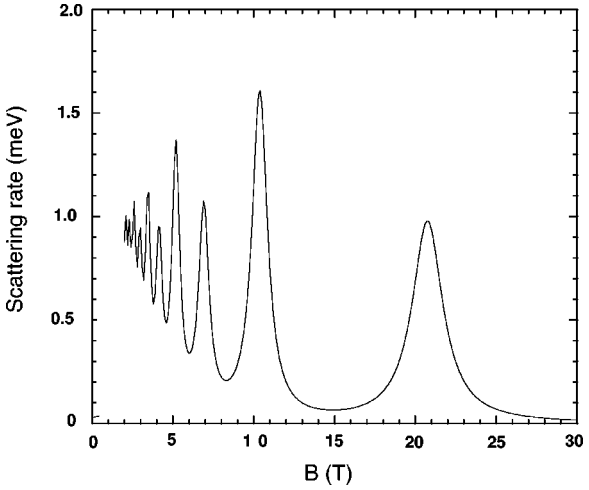

FIG. 1. Calculated scattering rate vs magnetic field.

If the occupied LL is partially filled, then the strength of the δ function [Eq. (15)] is to be multiplied by $\mu/\hbar\omega_c$. Then the total contribution to the scattering rate is given by

$$\gamma=\frac{4\pi}{\hbar}\sum_n\frac{\mu}{\hbar\omega_c}a_n\delta(2\Delta-n\hbar\omega_c). \tag{18}$$

For a typical structure, the scattering rate as a function of the applied magnetic field is displayed in Fig. 1, where the energy conserving delta functions are replaced by Lorentzians of width 2 meV, typical of experiments in quantum well structures.

The scattering rate is seen to be highly oscillatory, with wide regions of negligible scattering in the high B range. At smaller B, the oscillation amplitudes are diminished and the peaks are more and more closely spaced. The mean value seems to approach a definite limit as $B\to 0$. Figure 1 does not show the results beyond $n=9$ since the computation time increases rapidly with increasing n. However, we can analytically evaluate what that limit should be in our formalism.

The summation over n in Eq. (18) can be formally carried out by replacing the sum by an integral. This leads to

$$\gamma=\frac{4\pi}{\hbar}\frac{\mu}{\hbar\omega_c}a_n\frac{1}{\hbar\omega_c}\Big|_{n=2\Delta/\hbar\omega_c} \tag{19}$$

which can also be rewritten as

$$\gamma=\frac{\pi}{\hbar}\frac{\mu}{\Delta^2}(n^2a_n)\Big|_{n=2\Delta/\hbar\omega_c}. \tag{20}$$

In the limit $B\to 0$, we have $n\to\infty$, and thus we obtain the scattering rate at zero magnetic field from our formalism via Eq. (20) by evaluating the limit of (n^2a_n) as $n\to\infty$. This is displayed in Fig. 2 for two different structures.

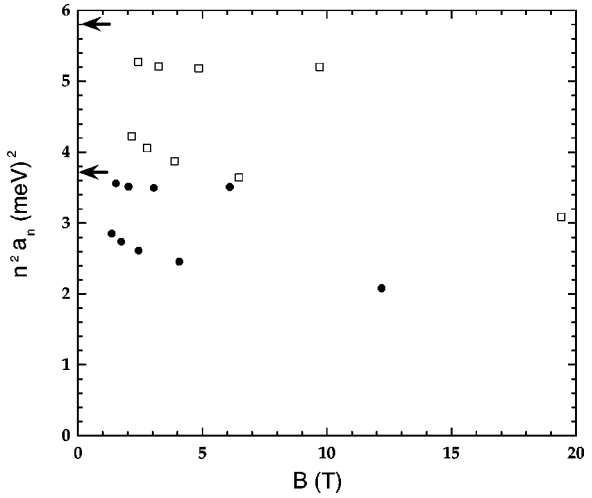

FIG. 2. Calculated values of n^2a_n vs magnetic field B for structures with two different intersubband separations (circles and squares). Arrows indicate the corresponding values in the zero magnetic-field limit.

In each case, the values of (n^2a_n) for odd and even n, fall on two different curves which show convergence to the same limit (for each respective case) as n goes to infinity. These agree well with our direct calculations for the scattering rates without any magnetic field, shown by the two arrows on the vertical axis. These direct calculations are based on our earlier formalism,[5] but using just the first two diagrams in the RPA expansion of the self-energy, instead of the full RPA, so as to correspond to the level of treatment here. This comparison serves as a physical benchmark test of our formalism. We also note that the two limits (indicated by the two arrows) are approximately in the ratio of the subband separations for the two cases displayed in Fig. 2.

The field-dependence in Fig. 1, resembles the Shubnikov–de Haas oscillations, however, we note that in Shubnikov–de Haas oscillations the (inelastic) scattering time is constant while the resistance oscillates with field due to modulation of the effective DOS as the Landau levels sweep through the Fermi energy. In Fig. 1, we plot the scattering due to *elastic* intersubband transitions between Landau levels of different subbands. The primary field dependence of the scattering rate is due to the B dependence of the energetic alignment of Landau levels of different subbands. In addition, we represent inelastic scattering by broadening the energy-conservation delta functions in Eq. (18) with a constant inelastic scattering rate in full analogy to the typical treatment of the Shubnikov–de Haas case.

IV. CONCLUSIONS

In this paper we have provided the detailed formalism for the study of the electron-electron scattering in strong magnetic fields in quantum well systems. We had already discussed a specific experiment[9,11] in our earlier publication,[9] and showed how the occurrence of peaks for odd n constitutes the signature of electron-electron scattering in a given structure. In that experiment, only the $n=1$ peak was visible, indicating weak electron-electron scattering processes compared to the single-electron processes.

The situation could change for structures and scenarios where higher currents flow and higher populations prevail in the active region. Since γ_{ee} scales with μ [Eq. (18)], the subband population, we could see a considerable enhancement of the odd peaks under these higher density scenarios. Since these contributions are only due to the two electron transfer scattering, we can quantitatively determine the subband populations by applying our formalism to analyze the experimental results. Based on that, we can also determine the electron-electron scattering contribution to even peaks. These are the processes like 2221, where only one electron changes the subband. Then subtracting this calculated amount from the total observed rates at the even peaks, we can determine the contribution of all the other (single-electron) scattering processes such as electron-surface scattering, electron-LO phonon scattering, etc.

All this can be extended to multisubband systems. Many more peaks occur (one complete series for each pair of subbands), and for smaller B there may not be sufficient resolution to identify these. However, for sufficiently large fields it may be possible to identify the $n=1$ and $n=2$ peaks for each pair of subbands. Such a situation allows us to obtain the detailed subband structure for a given system for each specific bias. One can also determine the subband populations from such data. It may be necessary to go beyond the treatment outlined here, to a full RPA calculation, to properly take into account the enhanced screening in the higher density situations.

Currently strong magnetic fields up to 50 T are available in the pulsed mode operation in a few laboratories. These suffice to study intersubband separations up to about 40 meV, in GaAs quantum wells. Even higher B fields in the pulsed mode can be obtained in special circumstances.

In this paper and in Ref. 9 we have provided an effective diagnostic technique for learning about the *in situ* scattering phenomena in actual experimental structures.

ACKNOWLEDGMENT

This work was supported in part by U.S. Army Research Office Grant No. DAAD 19-00-1-0108.

[1] G.D. Mahan, *Many-Particle Physics* (Plenum, New York, 1990).
[2] V. Fal'ko, Phys. Rev. B **47**, 13 585 (1993).
[3] P. Hyldgaard and J. Wilkins, Phys. Rev. B **53**, 6889 (1996).
[4] S.C. Lee and I. Galbraith, Phys. Rev. B **55**, R16 025 (1997).
[5] K. Kempa, P. Bakshi, J. Engelbrecht, and Y. Zhou, Phys. Rev. B **61**, 11 083 (2000).
[6] B.S. Williams, B. Xu, Q. Hu, and M.R. Melloch, Appl. Phys. Lett. **75**, 2927 (1999).
[7] M. Rochat, J. Faist, M. Beck, U. Oesterle, and M. Ilegems, Appl. Phys. Lett. **73**, 3724 (1998).
[8] K. Kempa, P. Bakshi, C.G. Du, G. Feng, A. Scorupsky, G. Strasser, C. Rauch, K. Unterrainer, and E. Gornik, J. Appl. Phys.

85, 3708 (1999); P. Bakshi, K. Kempa, A. Scorupsky, C.G. Du, G. Feng, R. Zobl, G. Strasser, C. Rauch, Ch. Pacher, K. Unterrainer, and E. Gornik, Appl. Phys. Lett. **75**, 1685 (1999).

[9] K. Kempa, Y. Zhou, J.R. Engelbrecht, P. Bakshi, H.I. Ha, J. Moser, M.J. Naughton, J. Ulrich, G. Strasser, E. Gornik, and K. Unterrainer, Phys. Rev. Lett. **88**, 226803 (2002).

[10] K. Kempa, P. Bakshi, J.R. Engelbrecht, and Y. Zhou, Physica E (Amsterdam) **7**, 225 (2000).

[11] J. Ulrich, R. Zobl, K. Unterrainer, G. Strasser, and E. Gornik, Appl. Phys. Lett. **76**, 19 (2000).